**The EMBO Journal (2012) 31,** 4057–4071 | © 2012 European Molecular Biology Organization | All Rights Reserved 0261-4189/12
www.embojournal.org

THE EMBO JOURNAL

# The Arf GAP ASAP1 provides a platform to regulate Arf4- and Rab11–Rab8-mediated ciliary receptor targeting

**Jing Wang[1], Yoshiko Morita[1], Jana Mazelova[1] and Dusanka Deretic[1,2,*]**

[1]Division of Ophthalmology, Department of Surgery, University of New Mexico School of Medicine, Albuquerque, NM, USA and [2]Department of Cell Biology and Physiology, University of New Mexico School of Medicine, Albuquerque, NM, USA

**Dysfunctional trafficking to primary cilia is a frequent cause of human diseases known as ciliopathies, yet molecular mechanisms for specific targeting of sensory receptors to cilia are largely unknown. Here, we show that the targeting of ciliary cargo, represented by rhodopsin, is mediated by a specialized system, the principal component of which is the Arf GAP ASAP1. Ablation of ASAP1 abolishes ciliary targeting and causes formation of actin-rich periciliary membrane projections that accumulate mislocalized rhodopsin. We find that ASAP1 serves as a scaffold that brings together the proteins necessary for transport to the cilia including the GTP-binding protein Arf4 and the two G proteins of the Rab family—Rab11 and Rab8—linked by the Rab8 guanine nucleotide exchange factor Rabin8. ASAP1 recognizes the FR ciliary targeting signal of rhodopsin. Rhodopsin FR-AA mutant, defective in ASAP1 binding, fails to interact with Rab8 and translocate across the periciliary diffusion barrier. Our study implies that other rhodopsin-like sensory receptors may interact with this conserved system and reach the cilia using the same platform.**

*The EMBO Journal* (2012) **31,** 4057–4071. doi:10.1038/emboj.2012.253; Published online 14 September 2012
*Subject Categories:* membranes & transport
*Keywords*: Arf GAPs; cilium; rabs; rhodopsin; trafficking

## Introduction

Primary cilia are specialized microtubule-based projections that are found on the cell membranes of almost all eukaryotic cell types. Defects in the formation and function of primary cilia affect multiple tissues and organs and cause a wide range of human diseases and developmental disorders, known as ciliopathies, which are characterized by both cystic kidneys and retinal degeneration and often combined with obesity, polydactyly and sensory impairments (Blacque and Leroux, 2006; Fliegauf *et al*, 2007; Gerdes *et al*, 2009; Sang *et al*, 2011). Formation and maintenance of primary cilia involves the precisely orchestrated targeting of specific proteins and lipids to the base of the cilia, followed by the transport across the periciliary diffusion barrier, which likely combines specific lipid ordering, Septin rings and transition zone protein complexes that control selective admission through the ciliary gate (Rosenbaum and Witman, 2002; Vieira *et al*, 2006; Leroux, 2007; Emmer *et al*, 2010; Hu *et al*, 2010; Nachury *et al*, 2010; Chih *et al*, 2012; Garcia-Gonzalo and Reiter, 2012).

Although their architecture varies, primary cilia are exquisitely organized for the capture of extracellular signals (Singla and Reiter, 2006). Sensory receptors are highly concentrated in ciliary membranes and together with other components of the signal transduction complexes they allow for extraordinary sensitivity to external stimuli. In the case of vision, they ensure the capture of a single photon of light via the unique light sensing organelle, the rod outer segment (ROS). ROS is a modified sensory cilium that houses rhodopsin, a prototypic G protein-coupled receptor (GPCR), and the associated phototransduction machinery. The ROS axoneme is filled with light sensitive disk membranes that are renewed throughout the lifetime of the cell (Insinna and Besharse, 2008). The axoneme originates in the rod photoreceptor cell body, the rod inner segment (RIS), where the endoplasmic reticulum (ER), the Golgi and the trans-Golgi network (TGN) are localized. The renewal of ROS membranes and the delivery of rhodopsin to the base of the cilium in the RIS are mediated by traffic intermediates known as rhodopsin transport carriers (RTCs; Deretic, 2010). This process is followed by the directional membrane flow to the ROS through the transitional zone, also referred to as the connecting cilium (Insinna and Besharse, 2008).

Previous studies have identified ubiquitous protein complexes controlling the morphology and traffic of key intracellular membranes; however, the regulation of the directionality of membrane flow to the specialized organelles such as the cilia remains unknown. Sorting of the ciliary cargo is regulated by protein adaptors or complexes that function as effectors of the Arf family of GTP-binding proteins (Kahn *et al*, 2006; Donaldson and Jackson, 2011). Two such complexes have recently been identified (Mazelova *et al*, 2009a; Jin *et al*, 2010). One of the complexes, named the BBSome because of its involvement in Bardet-Biedel Syndrome, functions as an effector of Arl6 at the base of the cilium and sorts the GPCR Sstr3 (Nachury *et al*, 2007; Jin *et al*, 2010). The other complex functions as an effector of Arf4 at the TGN, where it forms a targeting module comprised of (1) the Arf GTPase activating protein (GAP) ASAP1, (2) the small GTPase Rab11 and (3) the Rab11/Arf effector FIP3, which sorts rhodopsin into ciliary-targeted RTCs (Mazelova *et al*, 2009a). This complex serves many of the same functions as coat complexes, including regulation by a member of the Arf family, in this case it is assembled

*Corresponding author. Division of Ophthalmology, Department of Surgery, University of New Mexico School of Medicine, Basic Medical Sciences Building, Room 377, 915 Camino de Salud, NE, Albuquerque, NM 87131, USA. Tel.: +1 505 272 4968; Fax: +1 505 272 6029; E-mail: dderetic@salud.unm.edu

**Received: 19 April 2012; accepted: 14 August 2012; published online: 14 September 2012**

upon binding of Arf4 to the carboxyl terminal VxPx ciliary targeting motif of rhodopsin (Deretic *et al*, 1998, 2005). The highly conserved VxPx motif that regulates rhodopsin targeting and Arf4 binding is also functional in polycystins 1 and 2, and the cyclic nucleotide-gated channel CNGB1b subunit (Geng *et al*, 2006; Jenkins *et al*, 2006; Ward *et al*, 2011). Disruptions of the VxPx motif caused by mutations in the rhodopsin gene (http://www.retina-international.com/sci-news/rhomut.htm) lead to some of the most severe forms of autosomal dominant retinitis pigmentosa (ADRP; Bessant *et al*, 1999; Berson *et al*, 2002), suggesting a crucial role of this ciliary targeting module in photoreceptor homeostasis (Deretic, 2006). In addition to the VxPx motif, several ciliary targeting sequences have been identified, including a highly conserved FR motif that is also present in rhodopsin (Corbit *et al*, 2005). Divergent targeting sequences identified so far are likely to engage multiple binding partners that regulate ciliary targeting, and they probably act at multiple stages of membrane traffic (Corbit *et al*, 2005; Fan *et al*, 2007; Berbari *et al*, 2008; Kizhatil *et al*, 2009; Tao *et al*, 2009; Mazelova *et al*, 2009a; Follit *et al*, 2010; Jin *et al*, 2010).

The key component of the Arf4-based targeting complex, ASAP1, belongs to a family of multifunctional scaffold proteins that regulate membrane trafficking and actin remodelling (Randazzo and Hirsch, 2004; Nie and Randazzo, 2006). ASAP1 mediates GTP hydrolysis on Arf4, and functions as an Arf4 effector that regulates RTC budding (Mazelova *et al*, 2009a). A point mutation in Arf4 (I46D) selectively abolishes ASAP1-mediated GTP hydrolysis and disrupts RTC budding, causing rhodopsin mislocalization and rapid retinal degeneration in transgenic animals. ASAP1 contains the Arf GAP domain, pleckstrin homology (PH), SH3, proline-rich and N-terminal BAR domain (Randazzo and Hirsch, 2004; Nie and Randazzo, 2006). The BAR domain mediates membrane tubulation and homodimerization of ASAP1, and acts as an autoinhibitor of its GAP activity (Nie *et al*, 2006; Jian *et al*, 2009). Another component of the Arf4-based targeting module, the GTPase Rab11, has also been identified as a component of the ciliogenesis cascade (Knodler *et al*, 2010; Westlake *et al*, 2011), which parallels the yeast budding pathway (Ortiz *et al*, 2002).

In the present study, we show that the targeting of sensory receptors is highly conserved in ciliated cells. In this process, ASAP1 interacts in a hierarchical manner with the cargo and activated Arf4, and with the constituents of the ciliogenesis cascade: Rab11, the guanine nucleotide exchange factor Rabin8 (Hattula *et al*, 2002) and its target Rab8, which is a central regulator of polarized membrane traffic, carrier fusion and ciliogenesis (Deretic *et al*, 1995; Moritz *et al*, 2001; Nachury *et al*, 2007; Yoshimura *et al*, 2007; Kim *et al*, 2008; Omori *et al*, 2008; Tsang *et al*, 2008; Bryant *et al*, 2010; Murga-Zamalloa *et al*, 2010). Our findings reveal a principal role for ASAP1 in the specialized system for targeting of sensory receptors to primary cilia.

## Results

### *Rhodopsin is correctly targeted to primary cilia of kidney epithelial IMCD cells, in an ASAP1-dependent manner*

Because ASAP1 functions as an Arf4 GAP and an effector that regulates RTC budding, we sought to further define its role in the targeting of rhodopsin in ciliated cells. These studies were performed in the mouse inner medullary collecting duct (IMCD) cells because of the lack of retinal cell culture systems suitable for siRNA and transient protein expression, and because of the low transduction efficiency in intact mature retinal photoreceptors. We expressed in IMCD cells a fusion protein comprised of bovine rhodopsin followed by eGFP followed by the repeat of eight C-terminal amino acids of rhodopsin, which was necessary to preserve the accessibility of the VxPx targeting signal and ensure proper targeting of the protein (Figure 1A). The fusion protein used in our study (Rh-GFP-VxPx hereafter) was previously shown to correctly localize to cilia of hTERT-RPE1 cells (Trivedi and Williams, 2010). Moreover, a nearly identical rhodopsin fusion protein retained the wild-type phototransduction

**Figure 1** Rhodopsin is targeted to primary cilia of kidney epithelial IMCD cells, in ASAP1-dependent manner. (**A**) Schematic representation of the Rh-GFP-VxPx fusion protein. Structure of rhodopsin is presented as explained in Figure 3C. (**B**) IMCD3 cells transiently expressing Rh-GFP-VxPx were fixed, stained with antibody to acetylated tubulin and analysed by confocal microscopy. Three consecutive confocal 0.9 μm sections are presented. Rh-GFP-VxPx (green) and acetylated tubulin (Cy3, red) colocalize in the ciliary axoneme (yellow). Boxed area is magnified in the insets. Rh-GFP-VxPx is detected in the cilia tips (arrows). (**C**, **D**) IMCD3 cells were co-transfected with Rh-GFP-VxPx (green) and control siRNA (**C**) or ASAP1 siRNA (**D**). Representative images from two Z-stacks (shown in Supplementary Figure S1A and B) ascending towards the cilia are shown in (**C**) and (**D**). Boxed areas are magnified and shown in separate channels in the insets. XZ planes were taken along the yellow line and YZ planes along the perpendicular line that crosses through the cilium. (**C**) Rh-GFP-VxPx and acetylated tubulin colocalize in a cell transfected with control siRNA (yellow in merged, XZ and YZ, arrows in XZ). Arrows in insets indicate Rh-GFP-VxPx (green) localized at the tip of the cilium. (**D**) In a cell transfected with ASAP1 siRNA, Rh-GFP-VxPx is localized in a ring (green, arrows) around the cilium (red), from which a protrusion arises. In the XZ plane, Rh-GFP-VxPx filled protrusion (green, left arrow in XZ) is juxtaposed to the cilium (red, right arrow). In the YZ plane, Rh-GFP-VxPx (green) surrounds the cilium. (**E**) Ciliary localization of Rh-GFP-VxPx was determined in five separate experiments. The data were analysed using Student's *t*-test ($n = 5$, 5–15 cells in each experiment, a total of 40 cells for each condition) and presented as the means ± s.e.m. ($^{***}P < 0.0001$). (**F**) In a representative experiment, Rh-GFP-VxPx-acetylated-tubulin pixel colocalization analysis was performed within the cilia and expressed by the Pearson's coefficient ($n = 20$ cells each for control and ASAP1 siRNA) ($^{***}P < 0.0001$). (**G**, **H**): IMCD3 cells were co-transfected with Rh-GFP-VxPx (green) and control siRNA (**G**), or ASAP1 siRNA (**H**), and fixed cells were stained with phalloidin (blue) and the antibody to acetylated tubulin (red). (**G**) Rh-GFP-VxPx (green) and acetylated tubulin (red) colocalize in controls (yellow, arrow). Phalloidin staining (blue) is nearly undetectable around the cilium. (**H**) In ASAP1-depleted cells, Rh-GFP-VxPx (green) colocalizes with phalloidin (blue, light blue in the merged image) in the juxtaciliary protrusion (left arrow), but not with acetylated tubulin in the cilium (red, right arrow). Bar = 10 μm in (**B**); 5 μm in (**C**, **D**, **G** and **H**); 1 μm in the insets in (**C**) and (**D**). (**I**) Control siRNA-treated or ASAP1 siRNA-treated cells were lysed and proteins were separated by SDS–PAGE. Four different amounts of the control lysate were compared to the lysate from ASAP1 siRNA-treated cells. The expression of ASAP1 and Rab6 was examined by immunoblotting and quantified, as indicated in the figure, setting the control expression to 1. ASAP1 was diminished to ∼30% of control by siRNA treatment.

 

activity and localization in transgenic *Xenopus laevis* (Jin *et al*, 2003).

In IMCD3 cells, Rh-GFP-VxPx targeted to primary cilia, which were detected with an antibody to acetylated tubulin that labels the ciliary axoneme (Figure 1B, red). Confocal sections taken in ascending order towards cilia showed ciliary localization of Rh-GFP-VxPx, and its gradual accumulation at the tips of the cilia (Figure 1B, green, arrows in insets). IMCD3 cells transfected with control non-targeting siRNA were indistinguishable from non-silenced cells (Figure 1C; Supplementary Figure S1A). Rh-GFP-VxPx (Figure 1C, green) colocalized with acetylated tubulin present within the axoneme (Figure 1C, red, yellow in merged images; Supplementary Figure S1A and C). This colocalization was

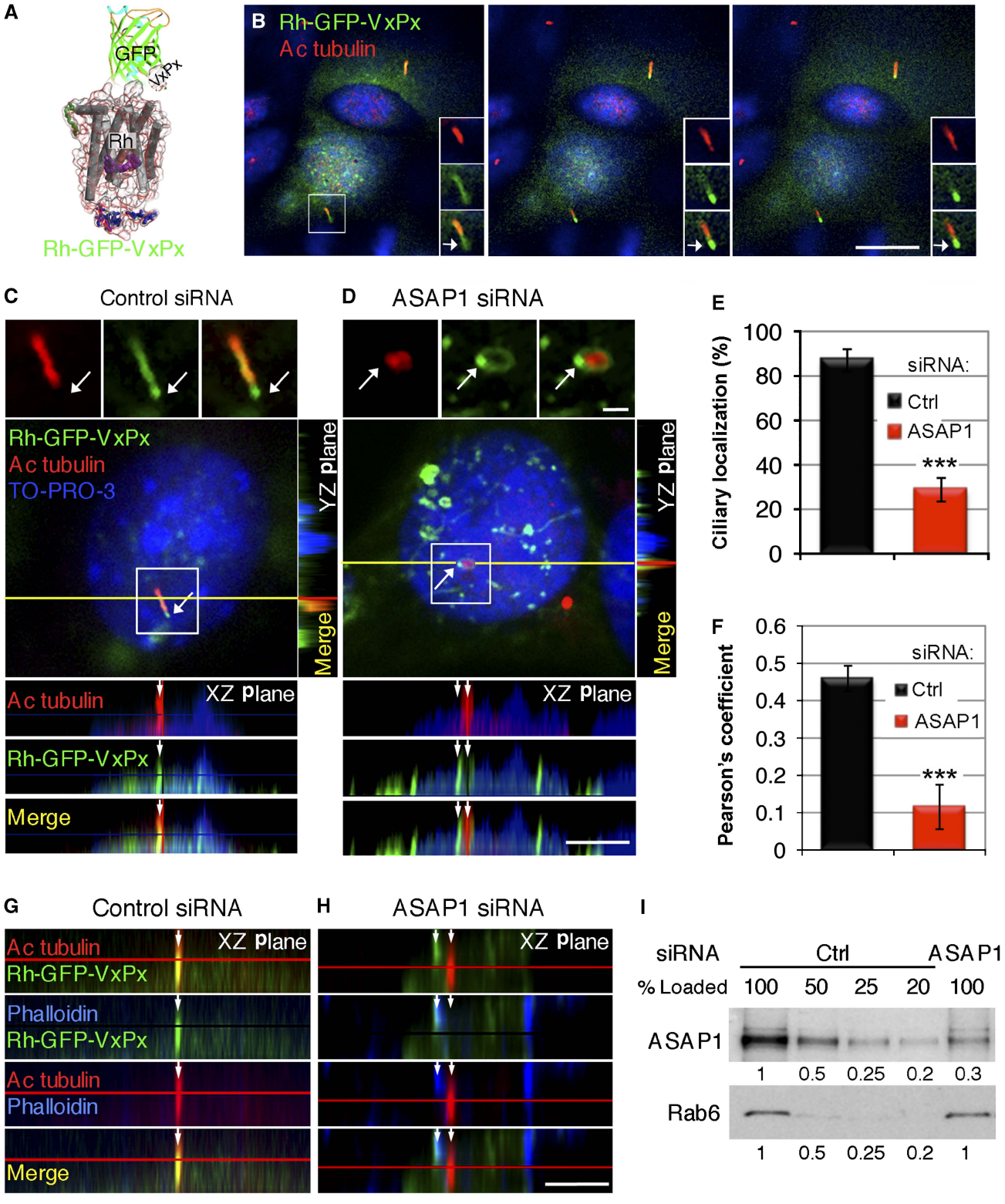

also visualized in the confocal XZ and YZ planes (Figure 1C, XZ, arrows, yellow in merged image; YZ, yellow). Again, Rh-GFP-VxPx (green) localized at the cilia tips devoid of acetylated tubulin (Figure 1C, arrows in insets; Supplementary Figure S1A, right arrows), indicating its entry into and transport along the ciliary membrane.

Depletion of ASAP1 did not affect the length of the primary cilia of IMCD3 cells ($3.94 \pm 0.26\,\mu m$ axoneme in control siRNA versus $3.78 \pm 0.25\,\mu m$ in ASAP1 siRNA-treated cells, $n = 16$). However, the ciliary localization of Rh-GFP-VxPx was profoundly altered. Nearly 40% of ASAP1-depleted cells displayed Rh-GFP-VxPx enriched rings around the cilia, which gave rise to ectopic membrane projections in the immediate vicinity of the cilia that accumulated mislocalized Rh-GFP-VxPx (Figure 1D, green, arrows in insets; Supplementary Figure S1B, arrows; Supplementary Figure S1D). Furthermore, Rh-GFP-VxPx (Figure 1D, XZ, green, arrows on the left; YZ, green) was absent from the cilium stained with an antibody to acetylated tubulin (XZ, red, arrows on the right; YZ, red). Whereas ~85% of the cells transfected with control siRNA correctly targeted Rh-GFP-VxPx, only ~30% of the cells treated with ASAP1 siRNA localized Rh-GFP-VxPx to primary cilia ($P = 4.47E^{-5}$) (Figure 1E). The pixel colocalization of Rh-GFP-VxPx with acetylated tubulin was significantly reduced in ASAP1-silenced cells ($P = 1.34E^{-5}$) (Figure 1F). Notably, control cells had relatively low Rh-GFP-VxPx-acetylated-tubulin pixel-by-pixel colocalization because of the predictable incomplete overlap of membrane-localized rhodopsin with axonemal acetylated tubulin. The ASAP1 siRNA resulted in a decrease of protein to ~30% of control levels, while having no effect on the expression of an unrelated protein Rab6 (Figure 1I). The correct targeting of Rh-GFP-VxPx in a small population of ASAP1 siRNA-silenced cells may be due to the residual expression of ASAP1 in ~30% of treated cells.

### *Rhodopsin is localized in actin-rich juxtaciliary protrusions in ASAP1-depleted cells*

Because ASAP1 is a known regulator of actin dynamics (Randazzo *et al*, 2000), we examined if actin reorganization was involved in the atypical membrane sprouting seen in ASAP1 siRNA-treated cells. We labelled control and ASAP1 siRNA-treated IMCD3 cells with phalloidin (Figure 1G and H). In control siRNA-treated cells, Rh-GFP-VxPx (Figure 1G, green) was correctly targeted to cilia labelled with acetylated tubulin (Figure 1G, red, arrow, yellow in merged images). Periciliary region of cells treated with non-targeting siRNA was devoid of actin filaments, as revealed by the negligible phalloidin staining (Figure 1G, blue). By contrast, in ASAP1 siRNA-silenced cells, Rh-GFP-VxPx (Figure 1H, green) colocalized with phalloidin-stained actin filaments (Figure 1H, blue, left arrow, light blue in merged images) in membrane projections adjacent to, but clearly separated from primary cilia containing acetylated tubulin (Figure 1H, red, right arrow).

### *Rhodopsin sequentially interacts with activated Arf4, ASAP1 and Rab11 during progression out of the Golgi/TGN and into ciliary-targeted carriers (RTCs)*

To further dissect the specific interactions that regulate ciliary membrane transport, we employed primary retinal photoreceptors that are particularly amenable to biochemical and morphological analysis as they generate a single major type of ciliary-targeted carriers, the RTCs. We examined the association of the Arf4-, ASAP1- and Rab11-based trafficking complex with rhodopsin as it transits out of the photoreceptor TGN and into post-TGN carriers (RTCs), as schematically depicted in Figure 2A. Post-nuclear supernatant (PNS) prepared from isolated retinas was fractionated on sucrose density gradients, following our standard protocol (Deretic and Mazelova, 2009). ASAP1 and Rab11 co-fractionated with both the Golgi/TGN-enriched membrane fractions (Golgi/TGN hereafter) and the RTCs, whereas Arf4 associated only with the Golgi/TGN (Figure 2B; Supplementary Figure S2A). The Golgi/TGN preparation that contained Arf4 was supplemented with the slowly hydrolysable GTP analogue GppNHp and used for immunoprecipitation experiments with antibodies specific for Arf4, ASAP1 and Rab11. Antibodies to Arf4 and Rab11 immunoprecipitated ASAP1 (Figure 2C), as also described previously (Mazelova *et al*, 2009a). Remarkably, in co-IP experiments antibodies to Arf4, ASAP1 and Rab11 also co-immunoprecipitated

**Figure 2** Arf4, ASAP1 and Rab11 sequentially interact with rhodopsin transiting from the Golgi/TGN into ciliary-targeted RTCs. (**A**) Diagram of a photoreceptor cell. Primary cilium elaborates the ROS. Golgi and the TGN are localized in the myoid region (M) of the RIS. RTCs that bud from the TGN are targeted to the cilium (arrow), through the ellipsoid region (E) filled with mitochondria. AJ, adherens junctions; BB, basal body; m, mitochondria; N, nucleus; Sy, synapse. (**B**) PNS isolated from one retina was fractionated on sucrose gradients and RTCs and Golgi/TGN membranes were analysed by immunoblotting (IB), as indicated. All antibodies were tested on a single blot. (**C**) Golgi/TGN membranes were subjected to immunoprecipitation (IP) with specific antibodies, or control IgG, bound to protein-A beads. Immunoprecipitates were analysed by IB, as indicated. ASAP1, Rhodopsin and Arf4 were detected on a single blot and all lanes come from the same gel. Rab11 was detected on a duplicate blot. (**D**) PLA was performed with a single antibody to ASAP1. No red fluorescence was detected. Retinal section was visualized by DIC and annotated as in (**A**). OLM, outer limiting membrane (comprised of AJs); ONL, outer nuclear layer; OPL, outer plexiform layer, containing photoreceptor synapses. Nuclei were stained with TO-PRO-3 (blue). (**E**, **F**) PLA was performed with an antibody to rhodopsin (**E**), or with antibodies to rhodopsin and a Golgi-associated protein G20 (**F**). No red fluorescence was detected, signifying absence of protein–protein interactions. (**G**) Rhodopsin–Arf4 interaction sites (red dots) were detected by PLA. The same experiment was repeated for (**H**) rhodopsin–ASAP1, (**I**) rhodopsin–Rab11, (**J**) ASAP1–Arf4 and (**K**) Rab11–ASAP1. (**L**, **M**) Rhodopsin–Arf4 PLA (red dots) was subsequently stained with antibody to the trans-Golgi marker Rab6 conjugated to Alexa Fluor 488 (green). Arrows in (**L**) indicate rhodopsin–Arf4 interaction sites juxtaposed to the trans-Golgi. Arrows in (**M**) indicate rhodopsin–Arf4 interaction sites (red) at the tips of the trans-Golgi cisternae (Rab6, green). (**N**) Quantification methodology is summarized on a rhodopsin–ASAP1 PLA. White dashed lines outline individual photoreceptors and the RIS/ROS border. Yellow dashed lines demarcate the border of the ellipsoid (E) and myoid (M) region of the RIS, which is detectable in the DIC image by the change in optical properties associated with the tight mitochondrial packing. Red dots within the myoid were counted as the Golgi/TGN interaction sites, whereas those in the ellipsoid were counted as RTC interaction sites. The image contains 1 μm bar from confocal software. C, cilia. Bar = 5 μm in (**D**–**K**); 1 μm in (**L**–**N**). (**O**) Red fluorescent signals were quantified as outlined in (**N**). The data from a representative experiment (one of three separate experiments) were expressed as a per cent of total interaction sites within the RIS, analysed using Student's *t*-test ($n = 62$) and presented as the means ± s.e.m. ($^{***}P < 2.27E^{-6}$). (**P**) A diagram summarizing Golgi/TGN and RTC interaction sites of rhodopsin with Arf4, ASAP1 and Rab11, as detected by co-IPs and PLA. Figure source data can be found with the Supplementary data.

 

rhodopsin from the Golgi/TGN preparation (Figure 2C). While specificity was striking in our co-IP experiments, we sought a second, independent assay of protein–protein interactions to confirm these findings.

We performed the proximity ligation assay (PLA) that has the specificity and sensitivity capable of revealing precise subcellular localization of stable and transient protein–protein interactions *in situ* (Soderberg *et al*, 2006). PLA is based on the dual recognition of a target protein complex by two primary antibodies detected by specific secondary antibodies attached to oligonucleotides. Oligonucleotides that are <16 nm apart guide the formation of circular DNA, which is amplified; the product is hybridized to fluorescently labelled oligonucleotides (excitation 598 nm) that generate an output in a form of red fluorescent dots of ~0.5 μm in size, which are visualized by microscopy. For the PLA, we took advantage of the layered structure of vertebrate retinas that are composed of neuronal cell bodies and synapses.

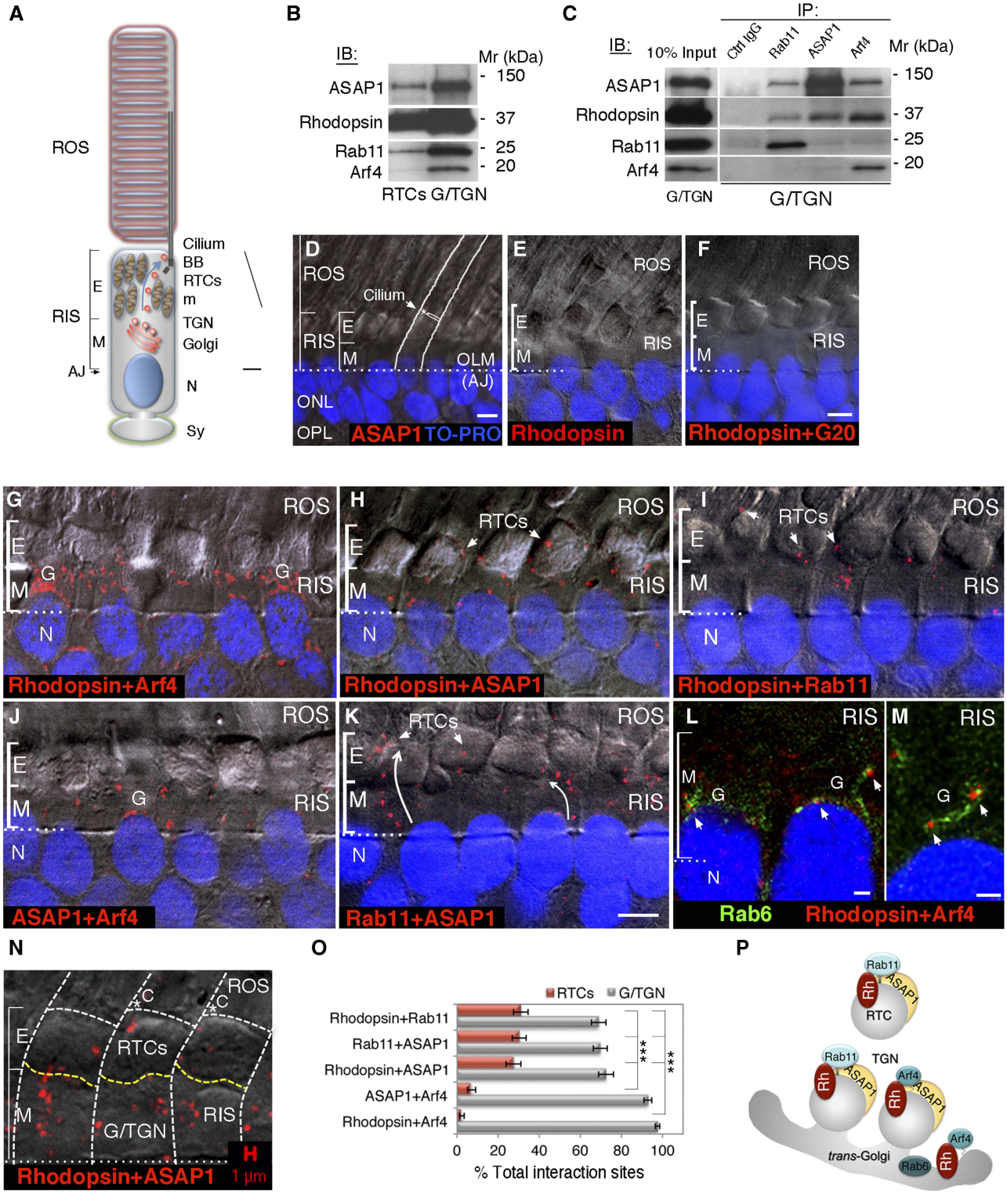

Retinal photoreceptor cells are well aligned and organized in a single retinal layer, which is readily identified by DIC and nuclear staining (Figure 2D) or with specific organelle markers (Supplementary Figure S2B–E). To investigate protein–protein interactions in 100 μm thick retinal sections by confocal microscopy, we employed the modified PLA adapted for brain slices (Trifilieff *et al*, 2011), which was also used in mouse retinas (Blasic *et al*, 2012). To establish the specificity of the assay, we determined that retinas treated with a single antibody to ASAP1 (Figure 2D), or rhodopsin (Figure 2E), showed no red fluorescent signal in the photoreceptor cell layer. Furthermore, rhodopsin showed no interactions with a control Golgi-associated protein G20 (Figure 2F), which was previously shown not to co-immunoprecipitate with the Arf4/ASAP1 complex (Mazelova *et al*, 2009a). Finally, ASAP1 showed no interaction with SNAP-25 (Supplementary Figure S2F), although it is partially localized in close proximity to the RIS plasma membrane that contains SNAP-25 (Mazelova *et al*, 2009a, b). Having established the specificity of the assay, we determined the localization of five different protein pairs detected in IP complexes described above. These are shown in Figure 2G–K and in Supplementary Figure S2G–K. As shown in Figure 2G and Supplementary Figure S2G, rhodopsin and Arf4 colocalized (red dots) almost exclusively in the Golgi area in the myoid region of the RIS. Rhodopsin colocalized with ASAP1 on the TGN-derived nascent buds, where we have localized ASAP1 previously (Mazelova *et al*, 2009a), as well as on RTCs that traverse the mitochondria-rich ellipsoid region en route to cilia (Figure 2H; Supplementary Figure S2H). Rhodopsin and Rab11 colocalized in the same region (Figure 2I; Supplementary Figure S2I). ASAP1 colocalized with Arf4 predominantly in the Golgi area (Figure 2J; Supplementary Figure S2J), and with Rab11 at the TGN and on RTCs (Figure 2K; Supplementary Figure S2K), consistent with our published report. To ascertain that the observed rhodopsin–Arf4 interaction sites were associated with the Golgi, following PLA we co-stained retinal sections with antibody to Rab6, which specifically detects the trans-Golgi cisternae (Mazelova *et al*, 2009a; Supplementary Figure S2D and E). Rhodopsin and Arf4 colocalized (arrows in Figure 2L and M; Supplementary Figure S2L and M) along the trans-Golgi cisternae stained with Rab6 (green). A fraction of the rhodopsin–Arf4-positive dots (red, arrows, Figure 2M; Supplementary Figure S2M) was observed at the tips of the trans-Golgi cisternae.

To quantify the number of specific interaction sites, we performed the count of red fluorescent signals within the ellipsoid and myoid regions of individual photoreceptors, as outlined in Figure 2N. We assigned the signals in the myoid region to the Golgi/TGN and in the ellipsoid region to RTCs because their localization within the RIS is well established. The number of interaction sites in a representative experiment was expressed as a per cent of total interaction sites within the RIS and is shown in Figure 2O. The per cent of rhodopsin–Arf4 interaction sites on RTC was negligible and significantly different from that for rhodopsin–ASAP1 ($P = 9.69E^{-10}$), rhodopsin–Rab11 ($P = 2.36E^{-12}$) and Rab11–ASAP1 ($P = 1.45E^{-12}$, $n = 62$ for all pairs). Likewise, the per cent of ASAP1–Arf4 interaction sites on RTCs was low and significantly different from the RTC interaction sites for rhodopsin–ASAP1 ($P = 2.27E^{-6}$), rhodopsin–Rab11 ($P = 2.26E^{-8}$) and Rab11–ASAP1 ($P = 2.29E^{-8}$, $n = 62$ for all pairs). These data indicate that interactions of rhodopsin and ASAP1 with Arf4 happen nearly exclusively at the Golgi/TGN, whereas rhodopsin–ASAP1–Rab11 interactions encompass the TGN-derived nascent buds and the RTCs, as schematically summarized in Figure 2P.

### *Rhodopsin forms a complex with Arf4 and ASAP1, which recognize its VxPx and FR ciliary targeting motifs, respectively*

Given that Arf4 directly binds to the VxPx motif of rhodopsin (Deretic *et al*, 2005), we asked whether the binding of ASAP1 to rhodopsin is also direct. For these experiments, we used recombinant 6His–ASAP1 BAR-PZA (Nie *et al*, 2006; Jian *et al*, 2009) (BAR-PZA hereafter), which contains the BAR, PH, Arf GAP and ankyrin repeat domains of ASAP1 (Figure 3A). We chose BAR-PZA because it fulfills functions as a GAP for Arf4 that stimulates RTC budding *in vitro* (Mazelova *et al*, 2009a). To examine the role of the BAR domain in rhodopsin interactions, BAR-PZA was first compared to the recombinant 6His–PZA, lacking the BAR domain (Supplementary Figure S3A and B). Using 6His pull-down assays, we tested rhodopsin–BAR-PZA or –PZA interactions in native Golgi/TGN membranes and RTCs mixed with cytosol (Supplementary Figure S3C). In both preparations, BAR-PZA pulled down rhodopsin significantly better than PZA ($P < 0.05$, $n = 3$), indicating that the BAR domain is important for rhodopsin–ASAP1 interactions.

Next, we performed 6His pull-downs of purified bovine rhodopsin with or without recombinant Arf4 pre-loaded with GppNHp, using BAR-PZA or the full-length ASAP1. BAR-PZA pulled down purified rhodopsin directly, significantly better than the 6His control ($P < 0.005$, $n = 3$) (Figure 3B). Arf4-GppNHp significantly stimulated direct rhodopsin–BAR-PZA binding ($P < 0.0002$, $n = 3$) resulting in a four-fold increase in rhodopsin bound to Ni-NTA beads (Figure 3B). Arf4-GppNHp also considerably enhanced binding of purified rhodopsin to full-length ASAP1, although this association appeared less efficient than binding to BAR-PZA (Figure 3B).

To examine if the VxPx motif also participates in binding of ASAP1 to rhodopsin, we tested if the monoclonal antibody 11D5, which binds the VxPx motif (Deretic *et al*, 2005) could inhibit the direct binding of recombinant ASAP1, or BAR-PZA, to purified bovine rhodopsin. In 6His pull-down experiments, mAb 11D5 surprisingly improved BAR-PZA pull down of purified bovine rhodopsin in the absence of Arf4 (Supplementary Figure S3D, compare to Figure 3B), indicating that the bound antibody had likely constrained the 3D structure such that BAR-PZA could more readily bind rhodopsin at a separate binding site. In the presence of Arf4, mAb 11D5 significantly inhibited interaction of BAR-PZA, both with rhodopsin ($P < 0.005$) and with Arf4, preventing the formation of the rhodopsin–Arf4–ASAP1 tripartite complex ($P < 0.005$, $n = 3$) (Supplementary Figure S3D). MAb 11D5 had no effect on the direct binding of Arf4 to ASAP1 in the absence of rhodopsin (Supplementary Figure S3E).

To determine the exact binding site of ASAP1 on rhodopsin, we surveyed the cytoplasmic surface of the crystal structure of rhodopsin (Palczewski *et al*, 2000). The C-terminal ciliary targeting VxPx motif lies in close proximity to the cytoplasmic α helix H-8, which contains another conserved ciliary targeting signal, known as the FR motif (Corbit *et al*, 2005; Figure 3C).

 

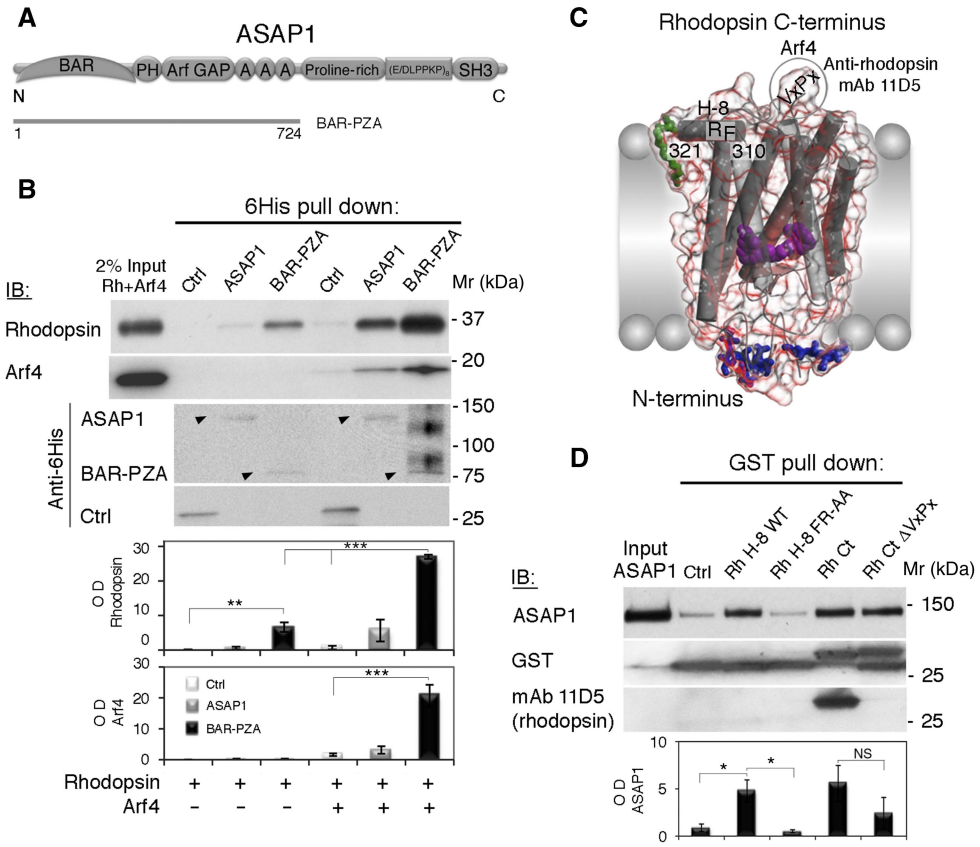


**Figure 3** ASAP1 recognizes the FR ciliary targeting motif of rhodopsin. (**A**) Schematic of ASAP1 with BAR-PZA (AA 1–724) indicated. (**B**) Recombinant 6His–ASAP1 (full-length), 6His–BAR-PZA or 6His control was incubated with purified bovine rhodopsin, with or without recombinant human Arf4 bound to GppNHp (5 μg of each protein). Rhodopsin and Arf4 bound to Ni-NTA agarose beads were detected by immunoblotting. The 6His-fusion proteins were detected with anti-6His antibody (arrowheads, rhodopsin trimers and tetramers are also visible). Rhodopsin monomer and Arf4 were quantified, the data were analysed using Student's *t*-test ($n=3$) and presented as the means ± s.e.m. (***$P<0.0005$; **$P<0.005$). (**C**) Schematic of bovine rhodopsin with protein backbone shown with a transparent surface, chromophore in purple, palmitic acid residues in green and oligosaccharides in blue (after Palczewski *et al*, 2000). The cytoplasmic C-terminal VxPx motif, which is the Arf4 binding site and also the antigenic site of mAb 11D5, is circled. The FR motif is within α helix H-8 (AA 310–321). (**D**) Rhodopsin peptides were expressed as GST-fusion proteins, as indicated, and incubated with 6His–ASAP1. Bound ASAP1 was detected with anti-ASAP1, whereas GST-fusion proteins were detected with anti-GST. GST-Rh Ct containing the VxPx motif is also detected by mAb 11D5. Bound ASAP1 was quantified exactly as in (**B**) (*$P=0.01$; NS, $P>0.05$). Figure source data can be found with the Supplementary data.

We therefore sought to determine if the FR motif of rhodopsin binds ASAP1. We compared the binding of ASAP1 to a GST-fusion protein containing the peptide corresponding to rhodopsin H-8 (AA 310-321) WT, or the rhodopsin H-8 FR-AA mutant. As shown in Figure 3D, ASAP1 bound rhodopsin H-8 WT and the FR-AA mutation abolished this interaction. We also tested ASAP1 binding to the GST-fusion protein containing rhodopsin C-terminal peptide (AA 327–354, RhCt) that was previously shown to bind Arf4 (Deretic *et al*, 2005) and the truncated fusion protein lacking the VxPx motif (AA 327–349, RhCt ΔVxPx) that does not bind Arf4. ASAP1 did not significantly discriminate between the two C-terminal fusion proteins, demonstrating that the VxPx motif is dispensable for rhodopsin–ASAP1 association (Figure 3D). This suggests that the cytoplasmic α helix H-8 and likely the membrane-proximal part of the C-terminal domain constitute at least a part of the ASAP1 binding site on rhodopsin.

### *Rhodopsin FR-AA mutant defective in ASAP1 binding fails to translocate across the periciliary diffusion barrier and to engage Rab8*

To test if the recognition of the FR signal by ASAP1 constitutes an obligatory step in ciliary targeting of rhodopsin, we generated the [FR-AA]Rh-GFP-VxPx mutant and examined its localization in IMCD3 cells. Rh-GFP-VxPx (green), which served as a control, localized in the ciliary membrane, including the cilia tips (Figure 4A–C, F and H, arrows in insets), as before. By contrast, the ciliary localization of the mutant [FR-AA]Rh-GFP-VxPx was completely abolished (Figure 4D, E, G and I and insets). Of the cells examined ($n=42$) 100% localized Rh-GFP-VxPx to the cilium, compared to 0% ($n=42$) of the cells expressing the FR-AA mutant. Analysis of pixel colocalization expressed by the Pearson's coefficient showed a negative correlation for [FR-AA]Rh-GFP-VxPx-acetylated tubulin, which was significantly different from that found for Rh-GFP-VxPx-acetylated tubulin ($P=4.46E^{-20}$) (Figure 4J). Furthermore, as depicted in Figure 4D, E and G, the area encircling the base of the cilium was remarkably devoid of the FR-AA mutant (arrows in insets). The rhodopsin-exclusion area around the cilium was 1.1 ± 0.1 μm ($n=8$), which is comparable to the size of the periciliary diffusion barrier of 1.2–1.8 μm (Vieira *et al*, 2006). [FR-AA]Rh-GFP-VxPx frequently accumulated at sites near the exclusion zone (Figure 4G and I, arrowheads in insets) that adjoined the cilium devoid of rhodopsin (Figure 4G and I, arrows in insets). Interestingly, this location

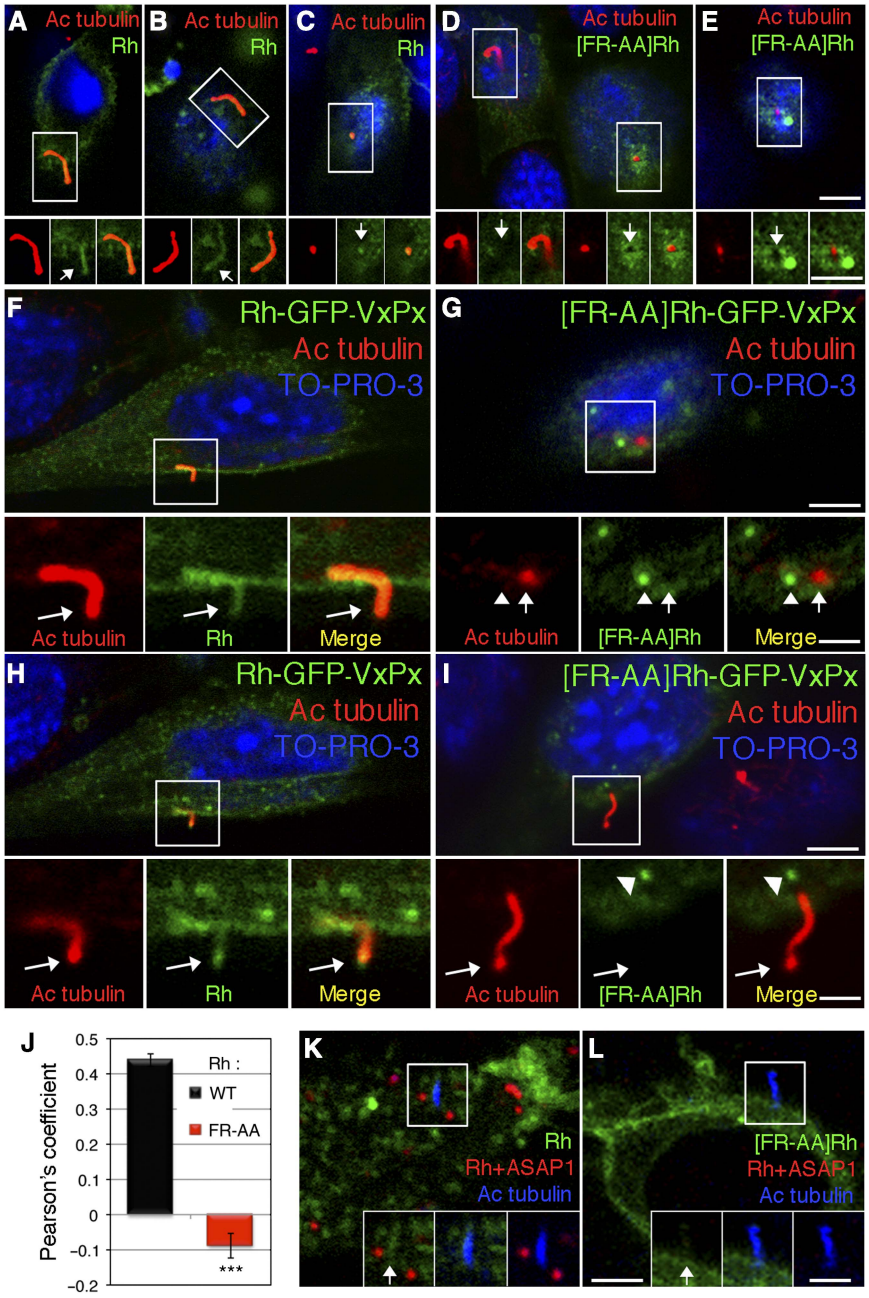


**Figure 4** Rhodopsin FR-AA mutant is deficient in ASAP1 binding and fails to translocate across the periciliary diffusion barrier. (**A–C**) IMCD3 cells transiently expressing Rh-GFP-VxPx were fixed, stained with antibody to acetylated tubulin and analysed by confocal microscopy. Confocal 0.9 μm sections are presented. Rh-GFP-VxPx (Rh, green) and acetylated tubulin (red) colocalize within the ciliary axoneme (yellow). Boxed areas are enlarged and shown in insets in separate channels and in merged images. Arrows in green panels point to Rh-GFP-VxPx in the ciliary axoneme. (**D**, **E**) IMCD3 cells transiently expressing mutant [FR-AA]Rh-GFP-VxPx ([FR-AA]Rh) were processed, as above. [FR-AA]Rh (green) is absent from the cilia. Boxed areas are shown in insets as in (**A–C**). Arrows in green panels indicate periciliary areas devoid of [FR-AA]Rh. (**F**, **H**) Two consecutive confocal sections of a cell expressing Rh-GFP-VxPx. Arrows in insets indicate colocalization of Rh with acetylated tubulin in the axoneme (**F**), and the cilia tips (**H**). (**G**, **I**) Confocal sections of two cells expressing [FR-AA]Rh-GFP-VxPx. (**G**) En face view of the primary cilium shows [FR-AA]Rh (green, arrowheads in insets) in a structure near the cilium (red, arrows in insets). The cilium is devoid of mutant rhodopsin and appears as a black hole, similar to that shown in (**E**). (**I**) [FR-AA]Rh (green) accumulates in the proximity of the ciliary base (arrowhead), but is excluded from the cilium (arrow). (**J**) Ciliary localization of Rh and [FR-AA]Rh was determined in five separate experiments ($n=5$, 5–16 cells in each experiment, a total of 42 cells for each condition). Rh-GFP-acetylated-tubulin pixel colocalization was expressed by the Pearson's coefficient. The data were analysed using Student's $t$ test ($n=5$) and presented as the means ± s.e.m. ($^{***}P=4.46E^{-20}$). (**K**) Rh-GFP-VxPx–ASAP1 interaction sites (red dots) were detected by PLA. (**L**) [FR-AA]Rh-GFP-VxPx-ASAP1 interaction sites were examined by PLA. No red fluorescence was detected. Bar = 5 μm in (**A–I**), (**K**), (**L**) and insets in (**A–E**), (**K**) and (**L**); 2 μm in insets in (**F–I**).

resembled the sites of outgrowth of the protrusions caused by the absence of ASAP1 (see Figure 1D). To further examine the direct interaction of rhodopsin with ASAP1, we compared the binding of Rh-GFP-VxPx, or the FR-AA mutant to ASAP1. As shown in Figure 4K, ASAP1–Rh-GFP-VxPx interaction sites visualized by PLA (red dots) were readily detectable through-

 

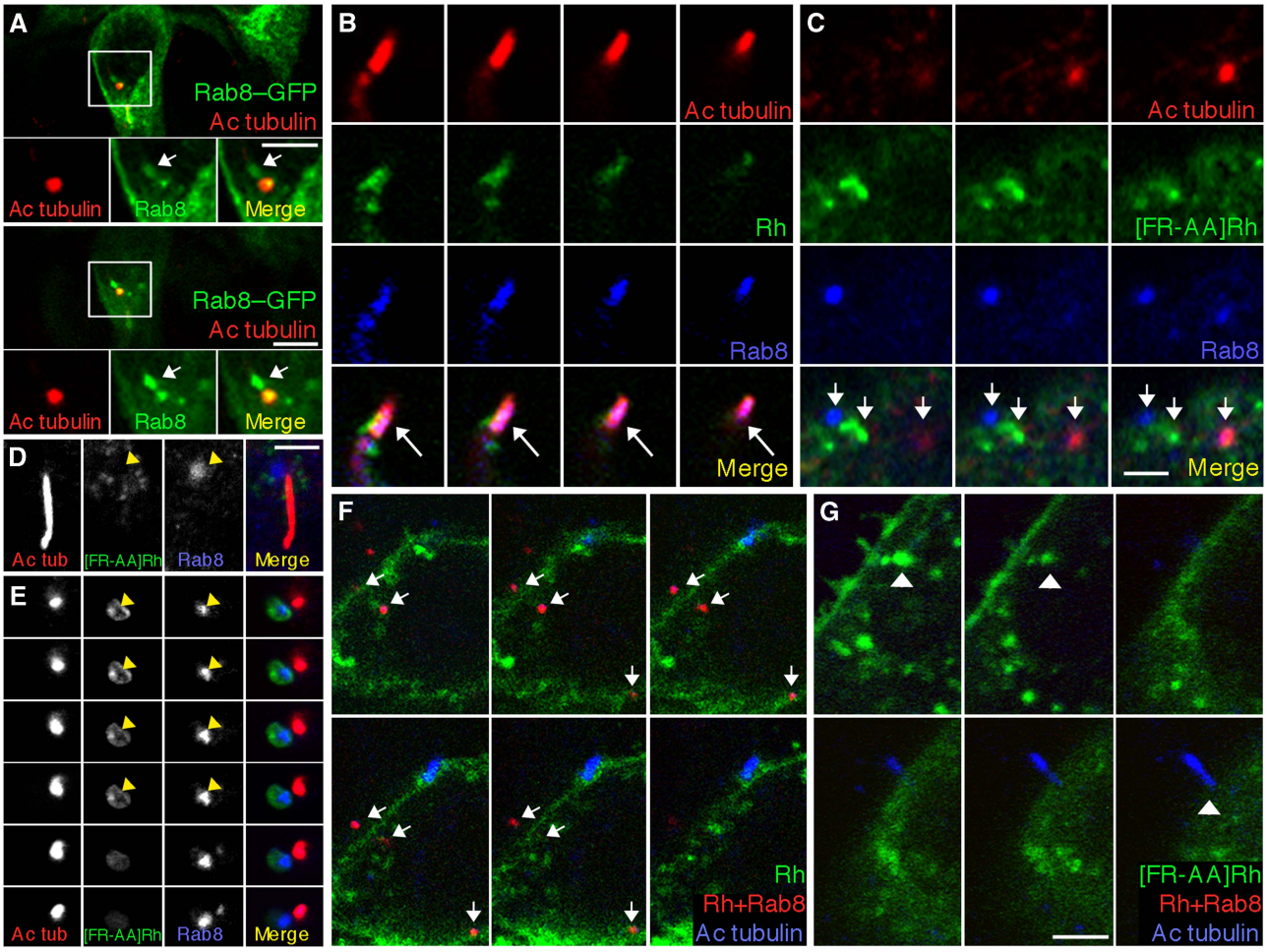


**Figure 5** Rhodopsin FR-AA mutant is excluded from the Rab8-positive periciliary structures. (**A**) Two consecutive confocal sections of IMCD3 cells expressing Rab8–GFP (green), which is localized to the periciliary foci (arrows) and also colocalizes with acetylated tubulin (red) in the ciliary axoneme (yellow in merged images). (**B**) Rh (green) colocalizes with acetylated tubulin (red) and Rab8 (blue) at the ciliary axoneme (arrow). (**C**) [FR-AA]Rh (green) localizes to a tubulo-vesicular structure that extends between the Rab8-positive structure (blue) and the cilium (Ac tub, red). Arrows in merged images indicate their discrete localization. (**D**) [FR-AA]Rh surrounds the Rab8-positive structure (yellow arrowhead) at the base of the cilium. (**E**) Doughnut-shaped [FR-AA]Rh-positive membranes envelop the Rab8-positive foci (yellow arrowheads) in the proximity of the cilium. (**F**) Six consecutive confocal 0.5 μm sections of a cell expressing Rh-GFP-VxPx are shown. Rh-GFP-VxPx–Rab8 interaction sites detected by PLA (red dots) distributed throughout the cell (arrows). (**G**) [FR-AA]Rh-GFP-VxPx–Rab8 interaction sites were examined by PLA. No red fluorescence was detected. [FR-AA]Rh-GFP-VxPx accumulated below the cilium (arrowheads). Panels 3–6 are four consecutive confocal 0.5 μm sections. Two single sections between panels 1 and 3 were omitted to better illustrate the site of accumulation of the [FR-AA]Rh mutant. Bar = 5 μm in (**A**), (**F**), (**G**) and insets in (**A**); 2 μm in (**B**–**E**).

out the cell and in the immediate vicinity of the cilium (arrow in inset). Colocalization was examined in three separate experiments. In a representative experiment, the average number of ASAP1–Rh-GFP-VxPx interaction sites per cell was $3.5 \pm 0.3$ ($n = 15$). By clear contrast, cells expressing [FR-AA]Rh-GFP-VxPx showed no red fluorescent signal (Figure 4L) and the number of interaction sites was 0 ($n = 15$), confirming that this mutant is indeed defective in ASAP1 binding.

Because Rab8 regulates rhodopsin trafficking (Deretic *et al*, 1995; Moritz *et al*, 2001), and Rab8–GFP localizes to cilia and a focal site below the cilium (Figure 5A, arrows in insets, see also Westlake *et al*, 2011), we considered the possibility that Rab8-postive foci are the site of accumulation of [FR-AA]Rh-GFP-VxPx. In the cilia of control cells, Rh-GFP-VxPx (Figure 5B, green) colocalized with acetylated tubulin (red) and Rab8 (blue, arrow in merged image). By contrast, the FR-AA mutant colocalized neither with acetylated tubulin nor with Rab8 (Figure 5C–E). Tubulo-vesicular structures containing [FR-AA]Rh-GFP-VxPx appeared to be extending between the cilia and the Rab8-positive (blue) foci (Figure 5C, arrows in merged image), encircling the Rab8-positive foci in the proximity of the cilia (Figure 5D, yellow arrowheads), or surrounding them in doughnut-shaped structures (Figure 5E, yellow arrowheads). We further tested rhodopsin–Rab8 interactions by serial confocal sections of IMCD3 cells analysed by PLA. Similarly to ASAP1, Rab8 bound Rh-GFP-VxPx throughout the cell (Figure 5F, arrows), but did not interact with [FR-AA]Rh-GFP-VxPx, which accumulated below the cilium (Figure 5G, arrowheads). In a representative experiment (one of three), the average number of Rab8–Rh-GFP-VxPx interaction sites per cell was $2.8 \pm 0.2$ ($n = 15$), whereas the number of interaction sites with the FR-AA mutant was 0 ($n = 15$). Collectively, these data indicate that the mutant rhodopsin defective in ASAP1 binding fails to engage Rab8 and translocate across the periciliary diffusion barrier for delivery to the primary cilium.

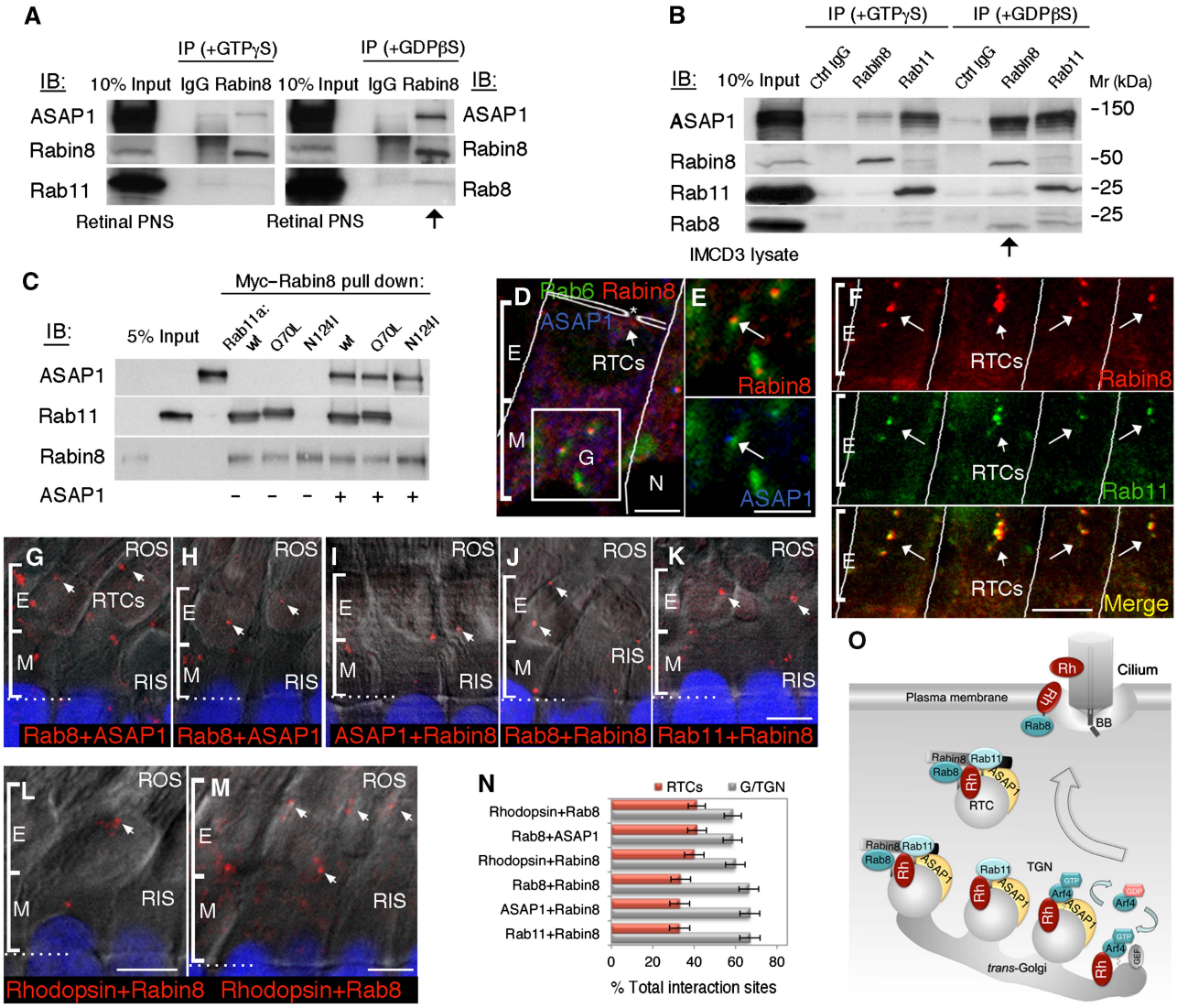


**Figure 6** ASAP1 acts as a scaffold for the Rab11a–Rabin8–Rab8 complex. (**A**) Anti-Rabin8, or the control IgG bound to protein-A beads was incubated with frog retina PNS and GTPγS, or GDPβS. Immunoprecipitates were analysed by immunoblotting, as indicated. Arrow points to the precipitate containing ASAP1, Rabin8 and $Rab8^{GDP}$. (**B**) Specific antibodies bound to protein-A beads were incubated with IMCD3 lysate, and precipitated proteins were detected on a single blot. The blot was sequentially probed with a polyclonal anti-Rab11, followed by a monoclonal anti-Rab8. Arrow points to the precipitate containing Rabin8, $Rab8^{GDP}$ and ASAP1. (**C**) Myc-Rabin8 bound to anti-Myc beads was incubated with Rab11aWT, Q70L or N124I mutant, with or without recombinant ASAP1. Bound proteins were detected by immunoblotting, as indicated. (**D**) A confocal optical section of the frog retina (0.9 μm). ASAP1 (blue) and Rabin8 (red) localize to the punctate structures associated with the trans-Golgi, revealed by Rab6 (green). Boxed area is magnified in (**E**). Cilium is indicated with an asterisk. (**E**) Magnified Golgi area from (**D**) is shown in separate channels to better visualize colocalization of Rabin8 and ASAP1 in nascent buds (arrows). (**F**) Rabin8 (red) colocalizes with Rab11 (green, yellow in merged image) on RTCs (arrows), traversing the mitochondria-rich ellipsoid area on the way to cilia. (**G**–**M**) Specific protein–protein interaction sites (red dots) were detected by PLA, as indicated in individual panels. Retinal sections were visualized by DIC. Nuclei were stained with TO-PRO-3 (blue). Specific protein–protein interaction sites are shown as follows: (**G**, **H**) Rab8–ASAP1, (**I**) ASAP1–Rabin8, (**J**) Rab8–Rabin8, (**K**) Rab11–Rabin8, (**L**) Rhodopsin–Rabin8 and (**M**) Rhodopsin–Rab8. Bar = 5 μm in (**F**–**M**); 2 μm in (**D**) and (**E**). (**N**) Red fluorescent signals were quantified as in Figure 2. The data from a representative experiment (one of three) were expressed and presented as in Figure 2 ($n = 62$). (**O**) Molecular interactions and the sequence of events likely taking place en route to cilia, as determined by our study.

### *Concomitant with RTC budding, ASAP1 acts as a scaffold for the Rab11a–Rabin8–Rab8 ciliary targeting complex*

Because Rab8 has been identified as a component of the ciliogenesis cascade, along with Rab11 (Bryant *et al*, 2010; Knodler *et al*, 2010; Westlake *et al*, 2011), we asked if ASAP1 is linked to the Rab11a–Rabin8–Rab8 ciliogenesis cascade. We first wanted to determine if Rab11a or Rab11b participates in the formation of the ciliary targeting complex with ASAP1. We predicted the involvement of Rab11a, since polyclonal anti-Rab11a (Lapierre *et al*, 2003) specifically recognized the endogenous photoreceptor protein (L Lapierre and J Goldenring, personal communication). We performed GST pull-down assays using purified proteins and reconstituted binding to bovine rhodopsin of recombinant human Arf4, Arf5 or Arf6, BAR-PZA, and GST-Rab11a or Rab11b, in the

presence of GppNHp. Rab11a bound rhodopsin directly, nevertheless Arf4 and BAR-PZA further enhanced their binding (Supplementary Figure S3F).

Next, we analysed the distribution of the Rab8 GEF Rabin8 in photoreceptor cells, by subcellular fractionation and confocal microscopy. Using the Rabin8 antibody (Hattula *et al*, 2002) that recognized the photoreceptor protein of ~50 kDa (Supplementary Figure S4B), we determined that Rabin8 is present on the photoreceptor Golgi/TGN and RTCs, as well as in the cytosol (Supplementary Figure S2A). We performed immunoprecipitation experiments from retina PNS supplemented with GTPγS or GDPβS (Figure 6A) using anti-Rabin8 antibody. We expected to observe the interaction of Rabin8 with $Rab11^{GTP}$ and $Rab8^{GDP}$, but found that Rab11 was not detected in the precipitates, likely due to antibody disruption of the $Rab11^{GTP}$–Rabin8 complex. Notably, anti-Rabin8 co-precipitated $Rab8^{GDP}$ along with ASAP1 (Figure 6A, arrow). Anti-Rabin8 also specifically precipitated ASAP1 from the RTCs (Supplementary Figure S4A, arrow), better than from the Golgi/TGN membranes. To confirm the direct interaction of $Rab11a^{GTP}$ and Rabin8, we performed Myc-Rabin8 pull-down experiments with recombinant Rab11a and ASAP1 (Figure 6C). Myc–Rabin8 pulled down Rab11a WT and the 'active' Rab11a Q70L mutant, but not the 'inactive' Rab11a N124I mutant (Figure 6C). When the full-length ASAP1 was also added, it was pulled down by Myc-Rabin8 regardless of the presence of WT or mutant Rab11a (Figure 6C). The Rab11a N124I mutant bound neither Rabin8 nor ASAP1. Importantly, the specificity of Myc-Rabin8 for the active form of Rab11a remained in the context of bound ASAP1, suggesting that Rab11a and ASAP1 separately bind Rabin8. We also examined the cell specificity of the Rabin8–ASAP1 interactions. Anti-Rabin8 precipitated ASAP1 along with Rab8 from IMCD3 cell lysates in the presence of GDPβS (Figure 6B, arrow), indicating that Rabin8–$Rab8^{GDP}$ associate with ASAP1 in other ciliated cells as well.

By confocal analysis of retinal sections that were not permeabilized before fixation, Rabin8 showed both cytosolic and membrane localization. Membrane-bound Rabin8 localized predominantly to ASAP1- and Rab11-positive nascent buds at the TGN and colocalized with Rab11 and Rab8 on RTCs (Figure 6D–F; Supplementary Figure S4C–I). Particularly striking colocalization of Rabin8 and Rab11 was observed on RTCs traversing the ellipsoid region (Figure 6F). Again, we examined protein–protein interactions by PLA, to confirm these findings. We determined the localization of the interaction sites of four different protein pairs detected in IP complexes (Figure 6G–K) and examined the interactions of Rab8 and Rabin8 with rhodopsin (Figure 6L and M). Notably, Rab8 and ASAP1 colocalized on RTCs and the TGN-derived nascent buds (Figure 6G and H, arrows indicate RTCs), as did ASAP1 and Rabin8 (Figure 6I), Rab8 and Rabin8 (Figure 6J), and Rab11 and Rabin8 (Figure 6K). Rhodopsin also colocalized with Rabin8 (Figure 6L) and with Rab8 (Figure 6M), in the same structures. We performed the count of fluorescent signals, as in Figure 2, to determine the number of interaction sites associated with the Golgi/TGN or RTCs. Quantification of the interaction sites in a representative experiment was expressed as a per cent of total within the RIS and is shown in Figure 6N. As these data were collected in a series of overlapping experiments with those presented in Figure 2O, we also performed the combined analysis, as shown in Supplementary Figure S4J. The per cent of Rab11–ASAP1 interaction sites on the Golgi/TGN was significantly higher than that for Rab8–ASAP1 ($P = 0.01$; Supplementary Figure S4J). Likewise, the per cent of rhodopsin–ASAP1 interaction sites on the Golgi/TGN was significantly higher than that for rhodopsin–Rab8 ($P = 0.01$, $n = 62$) (Supplementary Figure S4J). The distribution of interaction sites within the RIS (Supplementary Figure S4K) suggested that ASAP1–Rab11 complex is upstream of ASAP1–Rabin8–Rab8 complex. Furthermore, the number of interaction sites for Rab11–ASAP1 and Rab8–ASAP1 on the TGN showed significant differences ($2.39 \pm 0.18$ versus $1.56 \pm 0.14$, $P = 0.0004$), but on RTCs it was nearly equal ($0.94 \pm 0.08$ versus $0.95 \pm 0.09$, $P = 0.9$, $n = 62$), suggesting that the Rab8-containing nascent buds are likely the immediate precursors of RTCs. Interestingly, the number of rhodopsin–ASAP1 and rhodopsin–Rab8 interaction sites was comparable between the photoreceptors and IMCD3 cells, but they were grouped along the trans-Golgi in photoreceptor cells and dispersed throughout the IMCD3 cells. Collectively, our data indicate that the advancement of rhodopsin from the Golgi/TGN into post-TGN carriers proceeds in several stages and that the assembly of the ASAP1–Rab11a–Rabin8–Rab8 complex at the TGN is a crucial step in directing rhodopsin to the ciliary membrane. These findings also help explain why the rhodopsin FR-AA mutant defective in ASAP1 binding fails to interact with Rab8 and reach the primary cilium. Figure 6O outlines the sequence of events associated with the movement of rhodopsin to the primary cilia of photoreceptor cells, consistent with the results of our study. Although the ciliary pathway in photoreceptors is topographically more streamlined than in kidney epithelial cells, our data indicate that the molecular machineries and mechanisms regulating membrane delivery to the cilia are highly conserved.

## Discussion

Our study shows that the targeting of ciliary cargo, represented by rhodopsin, is mediated by sequential interactions with the regulatory complexes coordinated by Arf4 and the Arf GAP ASAP1. In these processes, ASAP1 acts as a scaffold that links the ciliary-targeted post-TGN carriers to the Rab11a–Rabin8–Rab8 complex to ensure their proper delivery to the cilium. ASAP1 recognizes the FR ciliary targeting motif of rhodopsin. Consequently, the FR-AA rhodopsin mutant defective in ASAP1 binding cannot engage Rab8 and fails to enter the ciliary membrane. Thus, ASAP1 likely is a key player in the directional movement of a subset of sensory receptors to the primary cilia.

The molecular interactions underlying the regulation of membrane targeting by ASAP1 are unclear at present. We demonstrate that the ciliary cargo sorting at the TGN involves a synergistic interaction of ASAP1 with Arf4 and rhodopsin. Arf4 is probably first activated at the trans-Golgi, by the Arf-GEF GBF1 (Szul *et al*, 2007). We find that activated Arf4 bound to rhodopsin's VxPx ciliary targeting motif significantly enhances the binding of ASAP1 to the second ciliary targeting signal, the FR motif, which is present in rhodopsin and other GPCRs (Corbit *et al*, 2005). The rhodopsin FR-AA mutant defective in ASAP1 binding does not localize to cilia and therefore is comparable to smoothened Ciliary Localization Deficient (CLDSmo)

mutant (Corbit *et al*, 2005). Interestingly, the GPCR Sstr3, which is the BBSome cargo, contains two neighbouring ciliary targeting motifs: the FK and the FR (Corbit *et al*, 2005). The FK motif is apparently not employed in the ciliary targeting of Sstr3 (Berbari *et al*, 2008); however, the function of the FR motif is unknown.

Phylogenic analysis of the structure and the architecture of membrane-deforming modules indicates that they essentially belong to three categories: protocoatomer-derived, ESCRT and BAR domain-associated complexes (Field *et al*, 2011). Our data indicate that the targeting of ciliary cargo presented in the context of Arf4 involves a stepwise assembly of ASAP1 BAR domain-associated complexes, unlike the ciliary sorting by the BBSome, which forms a protocoatomer-derived complex that functions 'en bloc', although it lacks the capacity to deform the membrane (Jin *et al*, 2010). ASAP1 regulates ciliary targeting through a ternary complex with Rab11a and the Arf/Rab11 effector FIP3 (Inoue *et al*, 2008; Mazelova *et al*, 2009a). Since ASAP1 and FIP3 act as homodimers, they may oligomerize to form a membrane-deforming protein coat. The differences in putative coats for ciliary targeting parallel the differences in the COPI and COPII coat protein complexes involved in bi-directional ER-Golgi trafficking (Lee *et al*, 2004). Some functions of ASAP1 resemble those of the Sec23 component of the COPII coat, which acts as a GAP for the Arf family GTPase Sar1, and controls the forward direction of vesicle traffic (Lord *et al*, 2011).

ASAP1 (also known as DDEF1, DEF1, AMAP1 and centaurin β4) is known to assemble a multitude of regulatory complexes involved in membrane-cytoskeletal interactions that affect membrane outgrowth, cell shape and motility. Its expression is highly regulated and the upregulation of ASAP1 has been linked to increased formation of cellular protrusions, cell spreading and the development of cancer (Lin *et al*, 2008; Sabe *et al*, 2009; Muller *et al*, 2010). Prolonged depletion of ASAP1 in cultured cells causes reduction of ciliated cell numbers (Kim *et al*, 2010). However, we found that the loss of ASAP1 does not directly block ciliogenesis, because cilia appear normal after short-term depletion. Rather, ASAP1 regulates ciliary access of specific components, so its prolonged depletion may cause the reduction in particular essential constituents, leading to the loss of cilia. Surprisingly, we found that the most prominent feature of the ASAP1-depleted cells is the formation of actin-rich periciliary membrane protrusions to which ciliary receptors are mistargeted. As actin dynamics also affect ciliation (Kim *et al*, 2010), our data suggest that ASAP1 may function at the ciliary base by integrating regulatory signals coordinating membrane traffic and cytoskeletal changes, possibly by preventing actin polymerization at the base of the cilia and providing ciliary access to membrane carriers. These functions are compatible with the structure of ASAP1 that likely evolved through accretion of many functional domains that cooperatively form a protein complex that orchestrates trafficking of specific membrane receptors. The assembly of other individual molecules fulfilling comparable functions may direct similar regulation in homologous trafficking pathways.

We believe that ASAP1 acts in ciliary traffic both as a scaffold for protein complex assembly and as a temporal regulator through GTPase hydrolysis of Arf4. We find that ASAP1–Rab11–Rabin8 complex is already formed at the Golgi/TGN, comparable to the Golgi association of Sec2p, the yeast counterpart of Rabin8 that is recruited cooperatively by phosphatidylinositol 4-phosphate (PI4P), and the Rab11 counterpart Ypt32 (Mizuno-Yamasaki *et al*, 2010). Our previous study (Mazelova *et al*, 2009a) suggested that Rab11 and ASAP1 were present on nascent post-TGN carriers, but that ASAP1 was absent from the periciliary RTCs, as inferred from two populations of Rab11-positive RTCs that differed in their buoyant density on sucrose gradients. We now believe that the low-density Rab11-positive-ASAP1-negative RTCs were a product of partial dissociation of peripherally associated membrane proteins such as ASAP1 and FIP3. Our current analysis by the exquisitely sensitive PLA shows unequivocally that ASAP1 persists both on periciliary RTCs and at the ciliary base in IMCD3 cells. It is important to note that although the molecular machineries and mechanisms regulating membrane delivery to the cilia appear to be conserved, there are distinct differences in the topography of the terminally differentiated photoreceptor cells and the IMCD3 cells used as a model in our studies. Photoreceptor cells are exquisitely adapted to accommodate an extreme case of efficient unidirectional ciliary receptor targeting. By contrast, the regulators of ciliary targeting in IMCD3 cells are not equally dedicated to the trafficking of the heterologously expressed rhodopsin. This is best exemplified by Rab8, which is mostly localized on RTCs in photoreceptors, but in IMCD3 cells appears to be associated with a separate periciliary compartment, possibly a recycling endosome, which transiently interacts with the ciliary targeted cargo, perhaps serving as a way station on the road to cilia (Garcia-Gonzalo and Reiter, 2012).

Our study indicates that ASAP1 serves as an affinity adaptor for spatially restricted activation of Rab8. The failure of a sensory receptor to engage the ASAP1-based scaffold would thus result in the inability of ciliary-targeted carriers to acquire Rabin8 and Rab8 and deliver cargo to the ciliary membrane. This is exactly what we observed with the rhodopsin FR-AA mutant. ASAP1 may control ciliary targeting by allowing only the cargo presented in the context of Arf4 to interact with Rab8 and pass across the periciliary diffusion barrier. We find that, in addition to ASAP1, rhodopsin also binds Rab11 and Rab8, similar to other ciliary sensory receptors (Follit *et al*, 2010; Ward *et al*, 2011). Both Rab11a and Rab8a interact with the Sec6/8 complex (Bryant *et al*, 2010) that also tethers the Rab11-positive membranes to midbodies during cytokinesis (Fielding *et al*, 2005). The Sec6/8 complex is localized at the base of the cilium in photoreceptors (Mazelova *et al*, 2009b) and in epithelial cells, consistent with its role as a tethering factor for ciliary-targeted carriers and an effector for the Rab11a–Rabin8–Rab8 ciliogenesis module responsible for membrane delivery to primary cilia. We find that once in the ciliary membrane, rhodopsin moves to ciliary tips, likely through the ubiquitous IFT machinery (Pazour *et al*, 2002; Rosenbaum and Witman, 2002; Bhowmick *et al*, 2009; Keady *et al*, 2011).

Recognition of the targeting signals and the correct delivery of sensory receptors to the ciliary membrane are processes that are adversely affected by mutations in rhodopsin that cause ADRP. Although the precise role of the interaction of the rhodopsin FR ciliary targeting signal with ASAP1

 

in retinal photoreceptors remains to be delineated, the data presented here implicate ASAP1 as an emerging key player in ciliary membrane biogenesis and compartmentalization of signalling receptors. Our studies provide a framework for the future investigation of molecular interactions that govern the biogenesis of cilia and cilia-derived sensory organelles and the involvement of the specific members of this machinery in ciliopathies and other human diseases.

## Materials and methods

### *Materials*

Mammalian expression vector encoding bovine rhodopsin eGFP was a kind gift of David Williams (UCLA). Purified bovine rhodopsin was a gift of Kris Palczewski (Case Western Reserve University). Primary antibodies used in this study were rabbit polyclonal anti-Arf4 (Mazelova *et al*, 2009a); anti-rhodopsin C-terminus mAb 11D5 (Deretic and Papermaster, 1991); monoclonal anti-ASAP1, anti-Rab8 and anti-Rab11 (BD Biosciences); rabbit polyclonal anti-ASAP1 (Randazzo *et al*, 2000), a gift of Paul Randazzo (NCI); rabbit polyclonal anti-Rab6 and goat polyclonal anti-Rab11 (Santa Cruz Biotechnology); mouse anti-acetylated tubulin (Sigma), goat anti-GST (Amersham Biosciences), rabbit anti-6His (Novus Biologicals) and mouse anti-6His (Qiagen). Rabbit polyclonal anti-Rabin8 (Hattula *et al*, 2002) and Myc-Rabin8 were gifts of Johan Peranen (University of Helsinki). Duolink II Rabbit/Mouse Red Kit (excitation: 598 nm; emission: 634 nm) was from Olink Bioscience.

### *Preparation of the photoreceptor-enriched PNS and retinal subcellular fractionation*

These experiments were performed according to established procedures that were recently described in detail (Deretic and Mazelova, 2009). Briefly, following pulse-chase labelling of isolated frog retinas, ROS were removed and retinal pellets were homogenized in 0.25 M sucrose and centrifuged at 1300 $g_{av}$, for 4 min to pellet the nuclei and retinal fragments. The PNS obtained after this centrifugation was further subfractionated by sedimentation followed by equilibrium sucrose gradient centrifugation. PNS was centrifuged at 17 500 *g*, for 10 min to obtain a pellet enriched in Golgi/TGN membranes. Resuspended Golgi/TGN-enriched membranes and the supernatant containing cytosol and RTCs were overlaid on two linear 20–39% (w/w) sucrose gradients and centrifuged at 100 000 $g_{av}$, for 13 h. Fourteen fractions were pooled into six pools, diluted and centrifuged at 336 000 $g_{av}$ for 30 min. To obtain purified RTCs, supernatant containing cytosol and RTCs was loaded on a step sucrose gradient and centrifuged for 90 min at 100 000 $g_{av}$. RTCs were recovered from the 20%/2.1 M sucrose interface and either pelleted or further fractionated on sucrose density gradients as described above.

### *Transfection of rhodopsin-eGFP WT and AA mutant*

Mouse IMCD3 cells were transiently transfected with a pcDNA™3.1 mammalian expression vector encoding bovine rhodopsin followed by eGFP followed by the repeat of eight C-terminal amino acids of rhodopsin (Rh-GFP-VxPx), or the rhodopsin FR-AA mutant ([FR-AA]Rh-GFP-VxPx), as described in Supplementary Methods.

### *Proximity ligation assay (PLA)*

Fluorescence assay was performed using Duolink II Rabbit/Mouse Red Kit (Olink Bioscience #92101) following manufacturer's protocol, with modifications as described (Trifilieff *et al*, 2011). Frog retinal sections were prepared as described in Supplementary Methods and incubated in blocking solution provided by the manufacturer for 1 h at RT. Sections were incubated with two primary antibodies overnight at 4°C. Two PLA probes were applied to samples and incubated overnight at 4°C. All washes were performed using buffers provided by the manufacturer. Ligases in ligation solution were added to samples and incubated for 1 h at 37°C, followed by the Amplification-Polymerase solution for 200 min at 37°C. Some samples were incubated with antibody to Rab6 conjugated to Alexa Fluor 488 and sections were counterstained with the nuclear stain TO-PRO-3. Confocal optical sections were generated as described in Supplementary Methods.

All other methods are described in Supplementary data.

### *Supplementary data*

Supplementary data are available at *The EMBO Journal* Online (http://www.embojournal.org).

## Acknowledgements

We thank Drs Kris Palczewski, Johan Peranen, Rytis Prekeris, Paul Randazzo and David Williams for their generous gifts of reagents and experimental advice and KP for the image of bovine rhodopsin. Supported by the NIH grant EY-12421. UNM Fluorescence Microscopy Facility is supported by NCRR, NSF, NCI and the UNM Cancer Center.

*Author contributions*: All authors planned the experiments and wrote the methods. JW performed pull-down and PLA experiments, generated [FR-AA]Rh-GFP-VxPx and analysed its expression, along with Rh-GFP-VxPx, in IMCD3 cells. YM performed pull-down and IP experiments and Rabin8 analysis. JM performed retinal subcellular fractionation and ASAP1 siRNA depletion in IMCD3 cells. DD performed the quantitative analysis and wrote the manuscript.

## Conflict of interest

The authors declare that they have no conflict of interest.

## References

Berbari NF, Johnson AD, Lewis JS, Askwith CC, Mykytyn K (2008) Identification of ciliary localization sequences within the third intracellular loop of G protein-coupled receptors. *Mol Biol Cell* **19:** 1540–1547

Berson EL, Rosner B, Weigel-DiFranco C, Dryja TP, Sandberg MA (2002) Disease progression in patients with dominant retinitis pigmentosa and rhodopsin mutations. *Invest Ophthalmol Vis Sci* **43:** 3027–3036

Bessant DA, Khaliq S, Hameed A, Anwar K, Payne AM, Mehdi SQ, Bhattacharya SS (1999) Severe autosomal dominant retinitis pigmentosa caused by a novel rhodopsin mutation (Ter349Glu). Mutations in brief no. 208. Online. *Hum Mutat* **13:** 83

Bhowmick R, Li M, Sun J, Baker SA, Insinna C, Besharse JC (2009) Photoreceptor IFT complexes containing chaperones, guanylyl cyclase 1 and rhodopsin. *Traffic* **10:** 648–663

Blacque OE, Leroux MR (2006) Bardet-Biedl syndrome: an emerging pathomechanism of intracellular transport. *Cell Mol Life Sci* **63:** 2145–2161

Blasic Jr JR, Lane Brown R, Robinson PR (2012) Light-dependent phosphorylation of the carboxy tail of mouse melanopsin. *Cell Mol Life Sci* **69:** 1551–1562

Bryant DM, Datta A, Rodriguez-Fraticelli AE, Peranen J, Martin-Belmonte F, Mostov KE (2010) A molecular network for *de novo* generation of the apical surface and lumen. *Nat Cell Biol* **12:** 1035–1045

Chih B, Liu P, Chinn Y, Chalouni C, Komuves LG, Hass PE, Sandoval W, Peterson AS (2012) A ciliopathy complex at the transition zone protects the cilia as a privileged membrane domain. *Nat Cell Biol* **14:** 61–72

Corbit KC, Aanstad P, Singla V, Norman AR, Stainier DY, Reiter JF (2005) Vertebrate Smoothened functions at the primary cilium. *Nature* **437:** 1018–1021

Deretic D (2006) A role for rhodopsin in a signal transduction cascade that regulates membrane trafficking and photoreceptor polarity. *Vision Res* **46:** 4427–4433

Deretic D (2010) Post-golgi trafficking and ciliary targeting of rhodopsin. In *Encyclopedia of the Eye*, Dartt DA (ed) Vol. 3, pp 480–487. Oxford, UK: Academic Press

Deretic D, Huber LA, Ransom N, Mancini M, Simons K, Papermaster DS (1995) rab8 in retinal photoreceptors may participate in rhodopsin transport and in rod outer segment disk morphogenesis. *J Cell Sci* **108**(Part 1): 215–224

Deretic D, Mazelova J (2009) Assay for *in vitro* budding of ciliary-targeted rhodopsin transport carriers. *Methods Cell Biol* **94:** 241–257

Deretic D, Papermaster DS (1991) Polarized sorting of rhodopsin on post-Golgi membranes in frog retinal photoreceptor cells. *J Cell Biol* **113:** 1281–1293

Deretic D, Schmerl S, Hargrave PA, Arendt A, McDowell JH (1998) Regulation of sorting and post-Golgi trafficking of rhodopsin by its C-terminal sequence QVS(A)PA. *Proc Natl Acad Sci USA* **95:** 10620–10625

Deretic D, Williams AH, Ransom N, Morel V, Hargrave PA, Arendt A (2005) Rhodopsin C terminus, the site of mutations causing retinal disease, regulates trafficking by binding to ADP-ribosylation factor 4 (ARF4). *Proc Natl Acad Sci USA* **102:** 3301–3306

Donaldson JG, Jackson CL (2011) ARF family G proteins and their regulators: roles in membrane transport, development and disease. *Nat Rev Mol Cell Biol* **12:** 362–375

Emmer BT, Maric D, Engman DM (2010) Molecular mechanisms of protein and lipid targeting to ciliary membranes. *J Cell Sci* **123**(Part 4): 529–536

Fan S, Fogg V, Wang Q, Chen XW, Liu CJ, Margolis B (2007) A novel Crumbs3 isoform regulates cell division and ciliogenesis via importin beta interactions. *J Cell Biol* **178:** 387–398

Field MC, Sali A, Rout MP (2011) Evolution: on a bender–BARs, ESCRTs, COPs, and finally getting your coat. *J Cell Biol* **193:** 963–972

Fielding AB, Schonteich E, Matheson J, Wilson G, Yu X, Hickson GR, Srivastava S, Baldwin SA, Prekeris R, Gould GW (2005) Rab11-FIP3 and FIP4 interact with Arf6 and the exocyst to control membrane traffic in cytokinesis. *EMBO J* **24:** 3389–3399

Fliegauf M, Benzing T, Omran H (2007) When cilia go bad: cilia defects and ciliopathies. *Nat Rev Mol Cell Biol* **8:** 880–893

Follit JA, Li L, Vucica Y, Pazour GJ (2010) The cytoplasmic tail of fibrocystin contains a ciliary targeting sequence. *J Cell Biol* **188:** 21–28

Garcia-Gonzalo FR, Reiter JF (2012) Scoring a backstage pass: Mechanisms of ciliogenesis and ciliary access. *J Cell Biol* **197:** 697–709

Geng L, Okuhara D, Yu Z, Tian X, Cai Y, Shibazaki S, Somlo S (2006) Polycystin-2 traffics to cilia independently of polycystin-1 by using an N-terminal RVxP motif. *J Cell Sci* **119**(Part 7): 1383–1395

Gerdes JM, Davis EE, Katsanis N (2009) The vertebrate primary cilium in development, homeostasis, and disease. *Cell* **137:** 32–45

Hattula K, Furuhjelm J, Arffman A, Peranen J (2002) A Rab8-specific GDP/GTP exchange factor is involved in actin remodeling and polarized membrane transport. *Mol Biol Cell* **13:** 3268–3280

Hu Q, Milenkovic L, Jin H, Scott MP, Nachury MV, Spiliotis ET, Nelson WJ (2010) A septin diffusion barrier at the base of the primary cilium maintains ciliary membrane protein distribution. *Science* **329:** 436–439

Inoue H, Ha VL, Prekeris R, Randazzo PA (2008) Arf GTPase-activating protein ASAP1 interacts with Rab11 effector FIP3 and regulates pericentrosomal localization of transferrin receptor-positive recycling endosome. *Mol Biol Cell* **19:** 4224–4237

Insinna C, Besharse JC (2008) Intraflagellar transport and the sensory outer segment of vertebrate photoreceptors. *Dev Dyn* **237:** 1982–1992

Jenkins PM, Hurd TW, Zhang L, McEwen DP, Brown RL, Margolis B, Verhey KJ, Martens JR (2006) Ciliary targeting of olfactory CNG channels requires the CNGB1b subunit and the kinesin-2 motor protein, KIF17. *Curr Biol* **16:** 1211–1216

Jian X, Brown P, Schuck P, Gruschus JM, Balbo A, Hinshaw JE, Randazzo PA (2009) Autoinhibition of Arf GTPase-activating protein activity by the BAR domain in ASAP1. *J Biol Chem* **284:** 1652–1663

Jin H, White SR, Shida T, Schultz S, Aguiar M, Nachury MV (2010) The conserved Bardet-Biedl Syndrome proteins assemble a coat that traffics membrane proteins to cilia. *Cell* **141:** 1208–1219

Jin S, McKee TD, Oprian DD (2003) An improved rhodopsin/EGFP fusion protein for use in the generation of transgenic Xenopus laevis. *FEBS Lett* **542:** 142–146

Kahn RA, Cherfils J, Elias M, Lovering RC, Munro S, Schurmann A (2006) Nomenclature for the human Arf family of GTP-binding proteins: ARF, ARL, and SAR proteins. *J Cell Biol* **172:** 645–650

Keady BT, Le YZ, Pazour GJ (2011) IFT20 is required for opsin trafficking and photoreceptor outer segment development. *Mol Biol Cell* **22:** 921–930

Kim J, Krishnaswami SR, Gleeson JG (2008) CEP290 interacts with the centriolar satellite component PCM-1 and is required for Rab8 localization to the primary cilium. *Hum Mol Genet* **17:** 3796–3805

Kim J, Lee JE, Heynen-Genel S, Suyama E, Ono K, Lee K, Ideker T, Aza-Blanc P, Gleeson JG (2010) Functional genomic screen for modulators of ciliogenesis and cilium length. *Nature* **464:** 1048–1051

Kizhatil K, Baker SA, Arshavsky VY, Bennett V (2009) Ankyrin-G promotes cyclic nucleotide-gated channel transport to rod photoreceptor sensory cilia. *Science* **323:** 1614–1617

Knodler A, Feng S, Zhang J, Zhang X, Das A, Peranen J, Guo W (2010) Coordination of Rab8 and Rab11 in primary ciliogenesis. *Proc Natl Acad Sci USA* **107:** 6346–6351

Lapierre LA, Dorn MC, Zimmerman CF, Navarre J, Burnette JO, Goldenring JR (2003) Rab11b resides in a vesicular compartment distinct from Rab11a in parietal cells and other epithelial cells. *Exp Cell Res* **290:** 322–331

Lee MC, Miller EA, Goldberg J, Orci L, Schekman R (2004) Bi-directional protein transport between the ER and Golgi. *Annu Rev Cell Dev Biol* **20:** 87–123

Leroux MR (2007) Taking vesicular transport to the cilium. *Cell* **129:** 1041–1043

Lin D, Watahiki A, Bayani J, Zhang F, Liu L, Ling V, Sadar MD, English J, Fazli L, So A, Gout PW, Gleave M, Squire JA, Wang YZ (2008) ASAP1, a gene at 8q24, is associated with prostate cancer metastasis. *Cancer Res* **68:** 4352–4359

Lord C, Bhandari D, Menon S, Ghassemian M, Nycz D, Hay J, Ghosh P, Ferro-Novick S (2011) Sequential interactions with Sec23 control the direction of vesicle traffic. *Nature* **473:** 181–186

Mazelova J, Astuto-Gribble L, Inoue H, Tam BM, Schonteich E, Prekeris R, Moritz OL, Randazzo PA, Deretic D (2009a) Ciliary targeting motif VxPx directs assembly of a trafficking module through Arf4. *EMBO J* **28:** 183–192

Mazelova J, Ransom N, Astuto-Gribble L, Wilson MC, Deretic D (2009b) Syntaxin 3 and SNAP-25 pairing, regulated by omega-3 docosahexaenoic acid, controls the delivery of rhodopsin for the biogenesis of cilia-derived sensory organelles, the rod outer segments. *J Cell Sci* **122**(Part 12): 2003–2013

Mizuno-Yamasaki E, Medkova M, Coleman J, Novick P (2010) Phosphatidylinositol 4-phosphate controls both membrane recruitment and a regulatory switch of the Rab GEF Sec2p. *Dev Cell* **18:** 828–840

Moritz OL, Tam BM, Hurd LL, Peranen J, Deretic D, Papermaster DS (2001) Mutant rab8 impairs docking and fusion of rhodopsin-bearing post-Golgi membranes and causes cell death of transgenic Xenopus rods. *Mol Biol Cell* **12:** 2341–2351

Muller T, Stein U, Poletti A, Garzia L, Rothley M, Plaumann D, Thiele W, Bauer M, Galasso A, Schlag P, Pankratz M, Zollo M, Sleeman JP (2010) ASAP1 promotes tumor cell motility and invasiveness, stimulates metastasis formation *in vivo*, and correlates with poor survival in colorectal cancer patients. *Oncogene* **29:** 2393–2403

Murga-Zamalloa CA, Atkins SJ, Peranen J, Swaroop A, Khanna H (2010) Interaction of retinitis pigmentosa GTPase regulator (RPGR) with RAB8A GTPase: implications for cilia dysfunction and photoreceptor degeneration. *Hum Mol Genet* **19:** 3591–3598

Nachury MV, Loktev AV, Zhang Q, Westlake CJ, Peranen J, Merdes A, Slusarski DC, Scheller RH, Bazan JF, Sheffield VC, Jackson PK (2007) A Core Complex of BBS Proteins Cooperates with the GTPase Rab8 to Promote Ciliary Membrane Biogenesis. *Cell* **129:** 1201–1213

Nachury MV, Seeley ES, Jin H (2010) Trafficking to the ciliary membrane: how to get across the periciliary diffusion barrier? *Annu Rev Cell Dev Biol* **26:** 59–87

Nie Z, Hirsch DS, Luo R, Jian X, Stauffer S, Cremesti A, Andrade J, Lebowitz J, Marino M, Ahvazi B, Hinshaw JE, Randazzo PA (2006) A BAR domain in the N terminus of the Arf GAP ASAP1 affects membrane structure and trafficking of epidermal growth factor receptor. *Curr Biol* **16:** 130–139

Nie Z, Randazzo PA (2006) Arf GAPs and membrane traffic. *J Cell Sci* **119**(Part 7): 1203–1211

 

Omori Y, Zhao C, Saras A, Mukhopadhyay S, Kim W, Furukawa T, Sengupta P, Veraksa A, Malicki J (2008) Elipsa is an early determinant of ciliogenesis that links the IFT particle to membrane-associated small GTPase Rab8. *Nat Cell Biol* **10:** 437–444

Ortiz D, Medkova M, Walch-Solimena C, Novick P (2002) Ypt32 recruits the Sec4p guanine nucleotide exchange factor, Sec2p, to secretory vesicles; evidence for a Rab cascade in yeast. *J Cell Biol* **157:** 1005–1015

Palczewski K, Kumasaka T, Hori T, Behnke CA, Motoshima H, Fox BA, Le Trong I, Teller DC, Okada T, Stenkamp RE, Yamamoto M, Miyano M (2000) Crystal structure of rhodopsin: a G protein-coupled receptor. *Science* **289:** 739–745

Pazour GJ, Baker SA, Deane JA, Cole DG, Dickert BL, Rosenbaum JL, Witman GB, Besharse JC (2002) The intraflagellar transport protein, IFT88, is essential for vertebrate photoreceptor assembly and maintenance. *J Cell Biol* **157:** 103–113

Randazzo PA, Andrade J, Miura K, Brown MT, Long YQ, Stauffer S, Roller P, Cooper JA (2000) The Arf GTPase-activating protein ASAP1 regulates the actin cytoskeleton. *Proc Natl Acad Sci USA* **97:** 4011–4016

Randazzo PA, Hirsch DS (2004) Arf GAPs: multifunctional proteins that regulate membrane traffic and actin remodelling. *Cell Signal* **16:** 401–413

Rosenbaum JL, Witman GB (2002) Intraflagellar transport. *Nat Rev Mol Cell Biol* **3:** 813–825

Sabe H, Hashimoto S, Morishige M, Ogawa E, Hashimoto A, Nam JM, Miura K, Yano H, Onodera Y (2009) The EGFR-GEP100-Arf6-AMAP1 signaling pathway specific to breast cancer invasion and metastasis. *Traffic* **10:** 982–993

Sang L, Miller JJ, Corbit KC, Giles RH, Brauer MJ, Otto EA, Baye LM, Wen X, Scales SJ, Kwong M, Huntzicker EG, Sfakianos MK, Sandoval W, Bazan JF, Kulkarni P, Garcia-Gonzalo FR, Seol AD, O'Toole JF, Held S, Reutter HM *et al* (2011) Mapping the NPHP-JBTS-MKS protein network reveals ciliopathy disease genes and pathways. *Cell* **145:** 513–528

Singla V, Reiter JF (2006) The primary cilium as the cell's antenna: signaling at a sensory organelle. *Science* **313:** 629–633

Soderberg O, Gullberg M, Jarvius M, Ridderstrale K, Leuchowius KJ, Jarvius J, Wester K, Hydbring P, Bahram F, Larsson LG, Landegren U (2006) Direct observation of individual endogenous protein complexes *in situ* by proximity ligation. *Nat Methods* **3:** 995–1000

Szul T, Grabski R, Lyons S, Morohashi Y, Shestopal S, Lowe M, Sztul E (2007) Dissecting the role of the ARF guanine nucleotide exchange factor GBF1 in Golgi biogenesis and protein trafficking. *J Cell Sci* **120**(Part 22): 3929–3940

Tao B, Bu S, Yang Z, Siroky B, Kappes JC, Kispert A, Guay-Woodford LM (2009) Cystin localizes to primary cilia via membrane microdomains and a targeting motif. *J Am Soc Nephrol* **20:** 2570–2580

Trifilieff P, Rives ML, Urizar E, Piskorowski RA, Vishwasrao HD, Castrillon J, Schmauss C, Slattman M, Gullberg M, Javitch JA (2011) Detection of antigen interactions *ex vivo* by proximity ligation assay: endogenous dopamine D2-adenosine A2A receptor complexes in the striatum. *Biotechniques* **51:** 111–118

Trivedi D, Williams DS (2010) Ciliary transport of opsin. *Adv Exp Med Biol* **664:** 185–191

Tsang WY, Bossard C, Khanna H, Peranen J, Swaroop A, Malhotra V, Dynlacht BD (2008) CP110 suppresses primary cilia formation through its interaction with CEP290, a protein deficient in human ciliary disease. *Dev Cell* **15:** 187–197

Vieira OV, Gaus K, Verkade P, Fullekrug J, Vaz WL, Simons K (2006) FAPP2, cilium formation, and compartmentalization of the apical membrane in polarized Madin-Darby canine kidney (MDCK) cells. *Proc Natl Acad Sci USA* **103:** 18556–18561

Ward HH, Brown-Glaberman U, Wang J, Morita Y, Alper SL, Bedrick EJ, Gattone 2nd VH, Deretic D, Wandinger-Ness A (2011) A conserved signal and GTPase complex are required for the ciliary transport of polycystin-1. *Mol Biol Cell* **22:** 3289–3305

Westlake CJ, Baye LM, Nachury MV, Wright KJ, Ervin KE, Phu L, Chalouni C, Beck JS, Kirkpatrick DS, Slusarski DC, Sheffield VC, Scheller RH, Jackson PK (2011) Primary cilia membrane assembly is initiated by Rab11 and transport protein particle II (TRAPPII) complex-dependent trafficking of Rabin8 to the centrosome. *Proc Natl Acad Sci USA* **108:** 2759–2764

Yoshimura S, Egerer J, Fuchs E, Haas AK, Barr FA (2007) Functional dissection of Rab GTPases involved in primary cilium formation. *J Cell Biol* **178:** 363–369